5-29-2013

Enhancing Remote Sensing for Agriculture Using Small Unmanned Aerial Systems: San Diego, CA, as a Test Case

Colin Kubera

Enhancing Remote Sensing for Agriculture using Small Unmanned Aerial Systems: San Diego, CA as a Test Case

Colin Kubera
Masters of Geographic Information Science
Department of Geography
The University of Denver
May 29, 2013

Abstract

The development of small Global Positioning System (GPS) antennas and microprocessors has propelled the advancement of affordable Small Unmanned Aerial Systems (SUASs), which will dramatically expand the remote sensing field, making timely, high-resolution imagery readily available. The low cost and simple operation of SUASs makes them an attractive option for agriculture. Flying a SUAS 400 ft above ground level (AGL) in a flight path that allows for significant image overlap can yield sub-5cm resolution imagery, which in turn can be mosaicked and used for multispectral imagery analysis. With results rivaling the most advanced commercial imaging sensors, SUASs can be used to identify stressed vegetation and aid in decision making that ultimately leads to more efficient farming practices and consistent yields. Furthermore, minimal operating costs promote reduced revisit times and enable persistent collection to monitor changes over time.

Table of Contents

List of Tables and Figures

Introduction

Precision agriculture is the nexus of Geographic Information Science (GIS) and agriculture that melds the two fields into one. By employing GIS in agriculture, farmers are able to efficiently track and monitor the pulse and ultimately the productivity of their crops. Precision agriculture encompasses everything from WiFi enabled sap sensors, to GPS guided tractors used to spray and harvest. While remote sensing is already a component of precision agriculture, it has remained too costly for most farmers to task collection for their own use, and instead may rely on government-funded programs. For those who have relied on the government imaging programs, collection remains too infrequent to fully leverage remote sensing's potential in the decision making process that drives modern farming. Further implementation of remote sensing will only enhance the information supporting precision agriculture, as it will assist in driving site specific monitoring, or rather the tracking of individual crops as distinct entities on a field instead of treating a field as one homogeneous unit (Michael 2010). By utilizing remote sensing in conjunction with other precision agriculture technologies, farmers stand better equipped to predict crop yields and therefore become proactive in their processes, resulting in more efficient applications of resources.

While California, and San Diego County in particular, is not conventionally thought of as an economic powerhouse of agriculture in the

United States, at the time of the last US census of agriculture in 2007, San Diego ranked 19th of 3,076 counties in the nation for the total value of agricultural products sold, and seventh for the total value of crops including nurseries and greenhouses (2007 Census of Agriculture 2007). San Diego has also long held the title of the avocado capital of the United states; however, its crown is already threatened as a continually expanding population in both the city and county makes land ever more scarce, and the sky-rocketing cost of water climbs even higher. Farmers may soon be forced to relocate elsewhere if operating costs become prohibitive to growing, but for those farmers who choose to remain rooted in San Diego, they will likely need to adopt or increase their reliance on the tools of precision agriculture to maximize the efficiency of their harvest and produce consistent yields.

Remote sensing could be an invaluable tool in delivering the information needed to keep the costs of irrigating, fertilizing, and pest control low, but it too will need to demonstrate that its benefits outweigh the costs before farmers consider depleting their constrained budgets on an additional tool. Since the majority of San Diego's farms are smaller than nine acres though, these small-scale operations are not conducive to traditional remote sensing because there are often minimum costs associated with collecting and analyzing the imagery that keep per-acre costs unaffordable unless hundreds to thousands of acres are imaged (San Diego Farm Bureau 2012). Smaller-sized farms like those in San Diego are

prime candidates for Small Unmanned Aerial Systems (SUASs) then due to their short flight times and negligible operating costs.

Capstone Goals

This project will demonstrate the advantages of using SUASs in remote sensing for agriculture, and will evaluate the performance of such platforms against existing satellite and airborne alternatives. In order to evaluate the performance, this paper will discuss system requirements, processing methods, and results from both testing and real-world employment.

Existing Remote Sensing Programs for Agriculture

NAIP

The National Agriculture Imagery Program (NAIP) began in 2001with the goal of collecting 1-meter color imagery of the entire United States to monitor land use and to verify that farm aid was being administered correctly, but now it has become widely used both within and outside of agriculture (USDA 2012). NAIP succeeded the National High Altitude Photography (NHAP) and National Aerial Photography Programs (NAPP), which collected images of the entire lower 48 contiguous states, in order to standardize collection and reduce duplicate effort (NHAP 2011). NAIP has an accuracy standard of less than six meters circular error, known as the CE95 value, or that 95% of verified points will fall within 6 meters of the value

indicated by the NAIP orthomosaic (USDA 2012). NAIP on the whole remains a highly cost effective program too, costing only about $13 per square mile for 1-meter collection, and $19 per square mile for half-meter collection (DOQQ 2009).

Despite the relatively low cost, even with higher resolution collection, the three-year revisit cycle still does little to aid an individual farmer in managing their crops when it comes to decision making. The low frequency of collection prevents NAIP as a whole from being a useful program for individual farmers. Remote sensing may never be a true substitute for in field sampling and verification of minerals, moisture, and plant health, but it is the best way to obtain a synoptic or macro level view of an area within the context of it's surroundings, and the only way to make such a synoptic perspective useful in the application of farming is to provide repeat collection over the course of a single growing cycle.

Sensor	Ground Sample Distance (resolution)	Typical Image Footprint	Band specifications
SUAS Operating Altitude: 120m Revisit rate: only weather limited	3 cm	112m x 84m	Blue(420-510nm) Green (460-590nm) Red (560-660nm) NIR (720-1000nm)
ADS40 Operating Altitude: Up to 7,260m unpressurized Revisit rate: cost limited	15 cm <240 KTS 30 cm <480 KTS 60 cm < 970 KTS	154m x 115m 307m x 230m 614m x 461m	Blue (430 – 490nm) Green (535 – 585nm) Red (610 – 660nm) NIR (835 – 885 nm) Panchromatic (465–680 nm)

Table 1.0.0: (Part I) Comparison of sensor specifications

WorldView 2 Operating Altitude: 770km Revisit rate: 1.1 days (1m GSD) CE90: 3.5m without GCPs	.5m (Panchromatic) 2m (Multispectral)	Large Area: 112km x 138km Long Strip: 360km x 16.4km Stereo: 112km x 63km Point : 16.4km x 16.4km	Panchromatic (450-800nm) Coastal Blue (400-450nm) Blue (450-510nm) Green (510-580nm) Yellow (585-625nm) Red (630-690nm) Red Edge (705-745nm) NIR (770-895nm) NIR2 (860-1040nm)
LandSat 7 ETM Operating Altitude: 705km Revisit rate: 16 days	15 m (band 8) 30 m (bands 1-5, 7) 60 m (band 6)	183 km x 170 km	Band1, blue (450-515nm) Band2, green (525-605nm) Band3, red (630-690nm) Band4, NIR (750-900nm) Band5, SWIR1 (1550-1750nm) Band6 Thermal IR (1040-1250nm) Band7 SWIR2 (2090-2350nm) Band8 Panchromatic (520-900nm)

Table 1.0.1: (Part II) Comparison of sensor specifications

Of the sensors used in NAIP, Leica's ADS40 is the one most commonly used. The ADS40 is a digital camera for airborne collection that captures three images simultaneously using a pushbroom method, in five separate bands (Blue, Green, Red, NIR, and Panchromatic). The pushbroom method (scanning along the direction of the flight path) allows the sensor to collect an image forward, nadir, and aft of the aircraft all at once, increasing image overlap, and minimizing the radial distortion of vertical objects (Lakehead University). The sensor's four multispectral bands (Blue, Green, Red, NIR) have discrete narrow regions within the electromagnetic spectrum that have no overlap and all have bandwidths less than 60nm, making the sensor ideal for multispectral analysis (Leica 2004). The ADS40 is also capable of recording 9 hours worth of imagery on its 580 GB hard drive at resolutions as high as 15cm and ground speeds as high as 240 KTS. It also combines the images with the exact location of the camera, as recorded by the Inertial Measurement Unit, logging the camera's motion and GPS capturing the

position. This highly accurate position is necessary in order to compile the images into a large orthomosaic (Lakehead University).

In 2003, the ADS40 was utilized for NAIP for the very first time. Within 90 days of starting collection, the contracted imaging companies were able to collect and process 90,000 square miles of farm land by flying two Cessna aircraft, each with an ADS40, for 90 hours over the course of 60 days, and then processing the images into color balanced mosaics in the remaining 30 days (Leica 2004). The early success with the ADS40 in the NAIP program made it a staple for subsequent years, and remains in use along side the newer ADS80.

Farmstar

France was an early adopter of remote sensing for agriculture through programs like Farmstar, leveraging satellite imagery to provide its subscribers with bespoke products and recommendations (Astrium EADS). Farmstar already has over 10,000 subscribers in France alone, and through the Farmstar program, image analysts can detect crop stress, assess the probable cause, and provide recommended solutions (Astrium EADS).

The value of stress detection and determination of cause is only valuable if collection is persistent and the time between acquisition to product dissemination and treatment is minimal. Rapid turnaround requires the analysis to occur near real time so that information retains its relevance and detected problems can be isolated. This persistent collection also

enables the Farmstar analysts to provide yield predictions, helping farmers ensure that their crops are developing as planned (Astrium EADS). Even though Farmstar has proven to be a highly successful program, the satellites it depends on are still challenged by weather, as clouds can prevent collection during key periods for extended lengths of time. Small UASs could someday prove to be an alternative collection platform during those times, since they have the ability to operate beneath the weather in localized areas.

Literature Review

Automated Photogrammetric Techniques on Ultra-light UAV Imagery

Using high-resolution photos acquired at low-altitude with metadata to georeference the images, the images can be stitched together using a method known as SIFT (Scale Invariant Feature Transform) to generate an orthomosaic (Strecha). Software like Pix4D, uses SIFT to automatically select matching points on the images to sew them together, and then merge them into a continuous surface. Since small UASs do not have high fidelity inertial positioning units like those found on traditional airborne sensors, software utilizing SIFT is necessary to provide acceptable levels of spatial accuracy. Testing has shown that SIFT can produce 2m accuracy using imagery acquired by UAS, and can be further enhanced by using Ground Control Points (GCPs) to increase the accuracy to .2m (Strecha).

An effective tool for generating tool for generating high quality orthomosaics is only beneficial if its derivative images produce valuable information for its end users. Pix4D provides a pain-free method for generating orthomosaics, but analysis of the images is still necessary in order to extract their full utility, which requires the use software like SOCET GXP and ArcGIS. By using SOCET GXP and existing orthomosaics such as NAIP, the accuracy of images mosaicked in Pix4D can be improved without the use of Ground Control Points, and with similar levels of accuracy that Dr. Strecha described in his paper. In order to perform effective multispectral analysis or to make the images useful over time in the role of change detection, the spatial difference between common features in the scene must be minimal.

Airborne Imaging for Foot Root Rot Detection

Using multispectral analysis and change detection enables farmers to have a comprehensive inventory of their crops, providing an assessment of current health, predictive yields, and historical context that aids in cementing those assessments and predictions. With that information in hand, farmers will be better suited to handle the environmental factors influencing their crops and help them to match and possibly even outperform those conditions. Although some farmers may not be interested in forcing every plant to its maximum potential with site specific management for irrigation or fertilization, the same is likely not true for coping with pests and

disease.

Even the simplest of multispectral image analysis techniques, visually interpreting color-infrared imagery, has proven to be an efficient means of detecting disease (Fletcher et al 2001, 94). Utilizing a citrus orchard known to have foot root rot present (Phytophthora parasitica, specifically), color-infrared imagery was acquired with an airborne sensor (Fletcher et al 2001, 94). The difference between healthy and infected trees was visually discernable by the depressed near infrared spectral reflectance of the infected trees as a result of lower foliar density, which was validated using a handheld spectrometer (Fletcher et al 2001, 96). The aerial imaging successfully confirmed the presence of mild foot root rot, however, the study does not demonstrate that this identification method would lead to detecting that the low vigor is specifically foot root rot alone. These observed symptoms could be attributed to another disease or infection, so even if similar lower reflectance values were observed in an area that was not previously identified with an infection, ground-truth measurements would be necessary in order to confirm an assessed infection of foot root rot.

Lastly, the test results do not divulge any specific NIR reflectance values that would be observed in the early stages of an infection. This is a significant shortcoming, because it is in the early stages of infection that treatment would likely be most successful at averting further damage and

economic loss. Detection in the early stages would be the most problematic as lower reflectance could be misinterpreted for early stages of draught or a lack of soil nutrients rather than a disease. This underscores the need for a thorough understanding of the plant's phenology, the history of the crops and their previous treatments, and the recent environmental factors affecting the crops in order to make an accurate assessment on health and possible infections by way of imagery analysis. Such crop and location-specific knowledge is necessary in order to evaluate when reflectance values have or are beginning to deviate from expected norms. Even though examining color-infrared has proven useful in identifying an infection, airborne imagery should only be categorized as a tool for indications and warnings before the crops can be examined in person, and a diagnosis made.

Remote Sensing of Vineyard Management Zones: Implications for Wine Quality

Remote sensing crops can be utilized to modify they way in which farmers approach field management, so that instead of treating one field as a homogenous entity, it is divided into sub blocks according to vigor, which in the case of vineyard management for wine making can contribute to improved consistency in quality of grapes and ultimately the value of a wine (Johnson et al 2001, 557). The study area was a vineyard in Napa,

California, that included high-quality clone and therefore consistent vines; however, the quality was not uniform due at least in part to the varied topography of the vineyard (Johnson et al 2001, 558). The vineyard was imaged using four-band imagery with a two-meter GSD that was then used to perform NDVI (Johnson et al 2001, 558). It was noted that the earth between vines was bare soil rather than grass or another form of undergrowth, but there is no further discussion about whether this is advantageous to remote sensing. Using the NDVI analysis, the field was divided into three categories of vigor: high, medium, and low. The grapes were then kept isolated by vigor category through fermentation and bottling (Johnson et al 2001, 559). Of the measurements taken throughout the process, in situ spectroscopy showed that there was negligible difference between the vigor categories with respect to chlorophyll concentration, but the difference in vigor was confirmed by differences in foliar biomass, which is measured by pruning weights (Johnson et al 2001, 558). As a result of the separating the grapes by vigor, that particular vineyard was able to produce a reserve quality wine for the first time.

By demonstrating modifications in management strategy based upon the information derived from remote sensing, the experiment was able to provide tangible evidence that sub-block vineyard management can have favorable results (Johnson et al 2001, 559). While top performing vineyards may be resistant to modify their farming strategies, those vineyards

producing more mediocre wines would benefit from incorporating remote sensing as a means of vectoring their grape selection for a particular wine. The dilemma for smaller or underperforming vineyards is that they may not have sufficient revenue available for satellite collection or traditional aerial imaging, or they may not be physically large enough to make either method appropriate, since both generally have cost minimums associated that are dictated by size. In this scenario where a small vineyard is seeking to adjust their management strategy, remote sensing with SUASs may be the conduit for information and analysis that was previously out of reach.

NDVI for yield prediction

A similar test was conducted by David Lamb to examine the effect of spectral resolution when imaging a cabernet sauvignon block (Lamb et al). By comparing image resolution at 20cm, 1m, and 3m for NDVI derived, Lamb conveys that there is significant data loss. And as discussed in the paper, the images may also show false patterns (Lamb et al). In the particular case shown the vine rows appear parallel with the bottom of the page; however, in the mid-resolution image, it appears to have streaks running 45^{o} to the vines that could lead to misinterpretation of vine vigor (Lamb et al). Lamb also identifies that by using a larger pixel size, data for canopies and shadows between rows is now merged, leaving a general trend of overall vigor, which in this case still appeared to correlate with the spatial

yield that was generated from harvest (Lamb et al). While it's imperative to be aware of potential miscues from the imagery, Lamb also points out the importance of when the imagery is taken, and in this case the imagery was collected at veraison, the period when grapes begin to ripen, and plants begin to put more energy into yielding fruit than growing leaves (Lamb et al). Lamb's works underscores the importance of having an in-depth understanding of the crops being imaged and their growing cycle in order correctly interpret and analyze the collected imagery. Even though Lamb demonstrates that NDVI can be useful in predicting yield when the results are generalized into a lower resolution product, such a loss is likely counterproductive for trying to pinpoint individual vines that are underperforming relative to their neighboring vines, which could also be an indicator of crop stress that requires treatment.

Early detection of crop stress is critical for providing consistent yield and quality fruit, and is therefore a fundamental component of precision agriculture. To get an accurate assessment of a plant's chlorophyll, and in turn health, its reflectance must be measured across the visible spectrum and into the near-infrared. Of particular interest is the red ledge or sharp rise at 700nm that occurs, because plants absorb energy at red wavelengths and reflect NIR. For green plants, this results in a large difference between red and NIR reflectance values when healthy, but that difference decreases significantly when stressed. By analyzing multispectral imagery that has

been acquired by a SUAS and stitched with SIFT, farmers will have a powerful tool for rapid and precise detection of stressed or endangered crops.

Objectives and System Requirements

In order for SUASs to be truly useful within agriculture, not only do they need to be affordable, but they also need to provide a service or information, which farmers do not currently have. Being airborne provides the SUAS sensors a unique perspective not otherwise available to farmers, particularly in the case of orchards, because the crowns of dense canopies cannot be observed from the ground. By using a sensor that is outside of the visible spectrum, it's possible to perform analysis of plant health because plants may reflect as much as 6x more energy in the near-infrared band (720-1000nm) than they do in the green band (550nm) (Statewide Mapping). Collecting the reflectance of near infrared (NIR) in addition to the standard red, green, blue bands that are used to capture the visible spectrum, allows for multiple forms of analysis. This research was focused on the implementing color infrared and Normalized Difference Vegetation Index (NDVI, calculated by (NIR-Red)/(NIR+Red)).

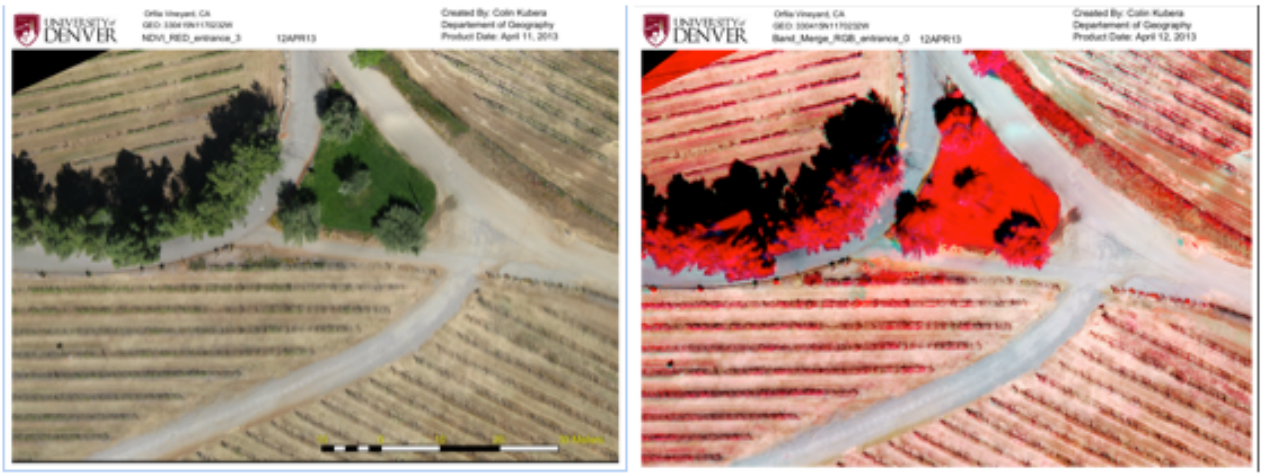

Image 2.0.0: Natural color and color IR images of Orfila Vineyard

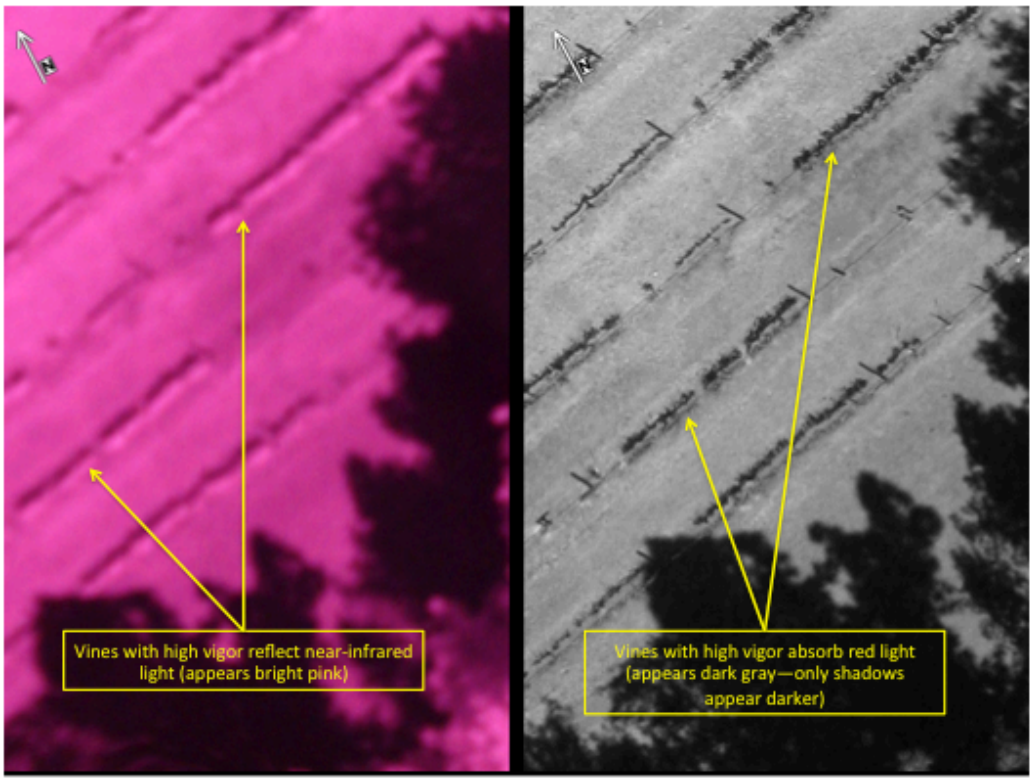

Image 2.1.0: Comparison of near infrared (NIR) and red components

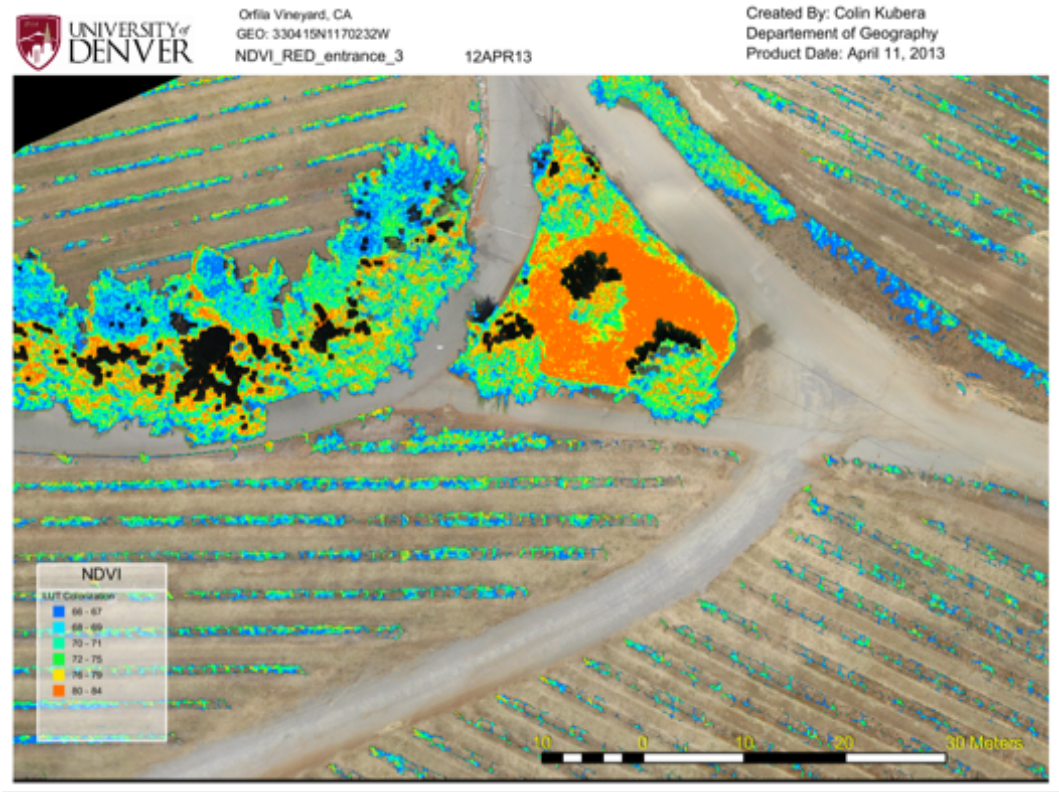

Image 2.2.0: Normalized Difference Vegetation Index (NDVI) output for the entrance of Orfila Vineyard

Vegetation Indices

NDVI is often accepted as the industry standard, but several other index methods exist for evaluating the health of vegetation. Of the simple indices, there is the Difference Vegetation Index (DVI= NIR-red), the Ratio Vegetation Index (RVI= NIR/red), and the Chlorophyll Index ($CI=(NIR_{880}/Vis_{590})-1$) (Jones 2010, 169). These simple calculations are susceptible to variances in lighting conditions though, which is why it is more common to use normalized indices (Jones 2010, 166). NDVI compensates for non-uniform lighting by factoring the total reflectance of NIR and red bands, rather than strictly measuring the difference between the two—calculated values range from -1 to 1, although SOCET GXP displays the

output in a range from 0-100. A similar measurement that has been adopted for dense vegetation is the Green Normalized Difference Vegetation Index (GNDVI), which substitutes red with green reflectance values in NDVI (Jones 2010, 167). Another common index used is the Soil Adjusted Vegetation Index (SAVI), which compensates for differing reflectance in the soil (Jones 2010, 169). SAVI is dependent on a user defined soil index (L) that is then added to modify the NDVI equation (SAVI=(1+L)(NIR-red)/(NIR+red+L)) (Jones 2010, 169). By default L is set to .5, but can be adjusted to better match the scene, but again, the adjustment is dependent on the user's understanding of the situation (Jones 2010, 169).

Regardless of which index method is used, all are subject to the effects of atmospheric attenuation, which suppresses and distorts the reflectance values received at the sensor, particularly in the case of satellites and high attitude airborne platforms (Jones 2010, 168). More advanced software applications for remote sensing incorporate atmospheric correction algorithms, which are necessary prerequisites to obtain results that can be used to make universal comparisons.

In the case of SUASs though, which operate at low altitudes, atmospheric effects are negligible. The biggest factor hindering consistent reflectance values for SUASs would be the presence of clouds, muting the reflectance of some or all of the target vegetation. Clouds could result in isolated shadows, transiting the collection area in the case of cumulus,

reduced total incident and reflected radiation in the case of high cirrus, or in the most extreme case, creating diffuse rather than direct lighting that drastically lowers incident radiation in the case of a dense stratus layer.

Capturing NIR

In order to capture near-infrared (NIR) energy, digital cameras need to be modified since their off-the-shelf configuration only captures visible light. The Charged Couple Device (CCD) sensors used by digital cameras are already sensitive to NIR light though, because they only rely on a filter between the lens and CCD to block NIR from reaching the CCD. This filter prevents visible light from being washed out by NIR, and keeps images appearing as the human eye perceives them. After removing the NIR filter, thereby making it sensitive to NIR, another filter must be installed to block visible light and only permit NIR to pass. A Hoya R72 is the ideal filter for this, since it only permits light of wavelengths longer than 720nm to pass and NIR energy, and because the CCD is only sensitive to 1000nm, the bandwidth for NIR is effectively 720nm to 1000nm, with band center at 860nm.

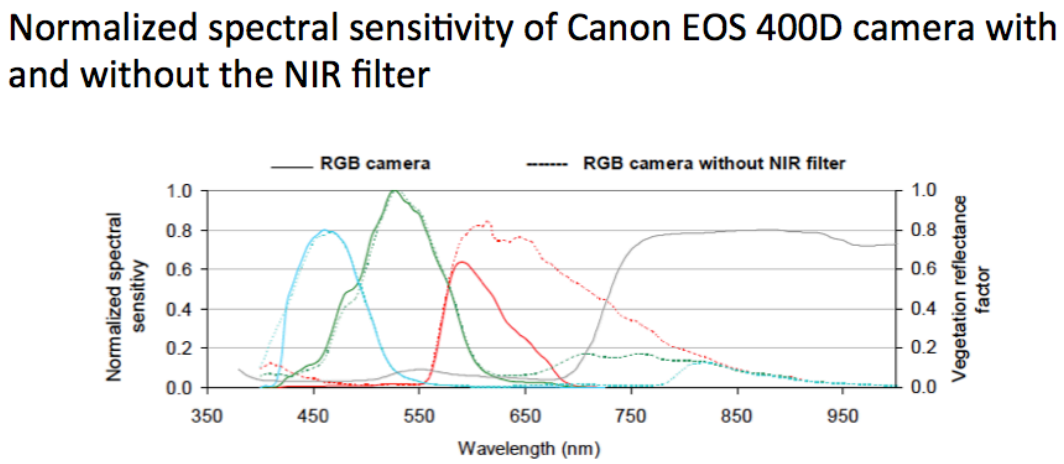

Chart 2.3.0: Spectral sensitivity of a Canon CMOS (rather than CCD as used in the project with the Canon A495) (Lebourgeois 2008, 7303).

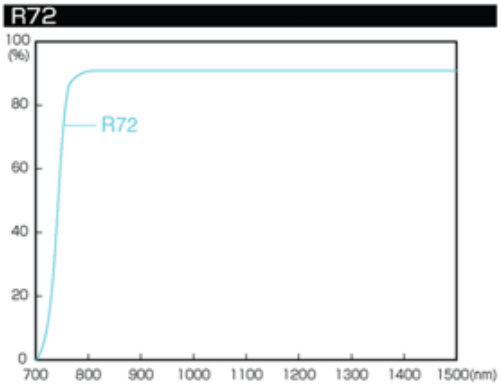

Chart 2.3.1: Spectral transmittance of a Hoya R72 Filter (Hoya Filters)

Platform Selection

The overall design selection of the SUAS platform was driven by the requirement to carry two cameras. This meant that the airframe had to generate sufficient lift and thrust to carry the weight of the cameras and the electronics required to operate the SUAS, while being controllable, reliable, and above all else, safe. Of suitable platforms, both fixed-wing and rotor-wing offer unique strengths and weaknesses. Although rotor/multi-rotor

platforms allow for operation in tight areas that would not otherwise be suitable for launch or recover of fixed-wing platforms that can collect imagery at extremely slow speeds, they aren't controllable in the event of a motor failure, unlike fixed-wing platforms that can continue to glide. Because fixed-wing platforms rely on a wing for lift, instead of rotors, they expend less energy required to cover the same distance, giving them greater range and the capability to cover larger areas.

Being able to carry two cameras dictated that the wing had to be quite large by RC-plane standards and have a large motor powerful enough to compensate for the added weight. Flying wings generate lift more efficiently than conventional, fuselage-based platforms. However, the tradeoff is that they offer minimal protection for downward facing cameras, even when internally mounted, since most do not have landing gear but instead land on the belly of the platform. By using a platform with a high mounted wing, there is considerably more protection for the cameras and electronics, while also meeting all other requirements. The only compromise is that a fixed wing platform still cannot match the takeoff and landing performance of a multi-rotor. Using the previously mentioned converted RC-plane, the goal was to successfully image 20-acres for multispectral analysis.

Challenges to SUAS Operations

Based upon the platform and its low operating altitude, there are several challenges to collecting usable, distortion-free, multispectral

imagery. Those challenges come in the form of vertical objects, terrain, and shadows.

Vertical objects influence SUAS operations by acting as obstructions to flight and by generating distortion in mosaics. In order to safely operate the SUAS, it is critical for a large enough launch-recovery area so that the SUAS can climb and descend with minimal risk of colliding with a tree or other obstruction, such as power lines. Trees in San Diego are commonly as tall as 70 feet, or 17.5% of the SUAS's collection altitude, and unless the camera is directly over top of the tree, the tree will appear to lean away on the image. In order to mitigate this appearance of leaning, redundant collection of the area of interest must be ensured and both cameras must be synchronized for near-simultaneous collection so that any lean will appear identically on both images.

Hilly and steep terrain can also be a significant contributor of distortion because varying elevation results in ground sample distances that are uneven over the scene of an image when the sensors are flown at a constant altitude. The impact of this was minimal in testing, but it is important to remember that the pixels at the bottom of a hill will cover a larger area than that at the top.

Shadows are always a factor, since there will always be some of the target vegetation that will be in the shadow, but because they can significantly alter the outcome of multispectral analysis, it is imperative to fly

at a time when shadow lengths are minimal. It is also critical that the NIR and red images are collected nearly simultaneously so that the shadow appears in the same location on both images. If the shadows do not align on both images, the output analysis will contain spurious results that could lead to incorrect conclusions regarding plant health and vigor.

Testing

Testing the system required a crawl, walk, run approach since RC-plane experience was low when starting the project. The defining requirement for the plane was that it needed to be capable of carrying two cameras, thereby needing sufficient thrust and lift, while also being able to fly slow enough for the cameras to capture images without being distorted by the minimum speed necessary to keep the plane flying straight and level. Testing and system development was refined through six phases over the course of six and a half months:

1. Flight testing—from basic handling and airworthiness to operating with a payload on a basic mission profile

2. Camera integration—successfully using the cameras on the ground and eventually mounting them to the fuselage

3. First Phase Processing—modifying the images and compiling them into mosaics so that they can be used in SOCET GXP and ArcGIS

4. Multispectral Analysis—first using satellite imagery as a test for how to conduct analysis, and then using images from flight testing

5. Final Testing—simulated operations over a defined area of interest to collect within while not having any gaps, and minimalizing image distortion.

6. Real World Employment—using the system over a farm (with permission) to validate the collection and results.

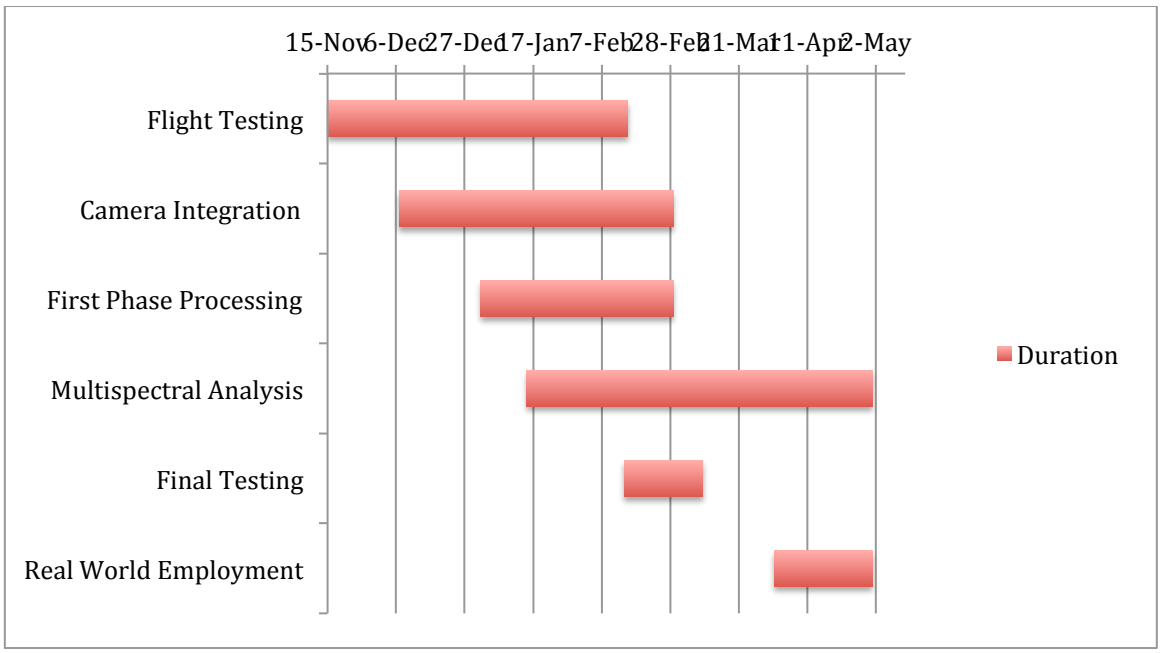

Chart 3.0.0: Project timeline

During the camera integration phase, it was quickly realized that maximizing image overlap was a priority. Because the critical limitation of the image overlap was the intervalometer script running the cameras, maxing out at only a 3 second interval, the solution was to slow the aircraft as much as

possible, while still having sufficient airspeed to maneuver, and to increase altitude, thereby increasing the image footprint.

Spatial Accuracy

While in the first phase processing component of testing, Microsoft's open source panoramic image stitching application, Image Collaborative Environment (ICE), was used to compile the mosaics to evaluate whether the project could remain within the open source realm, thereby becoming extremely affordable. Unfortunately though, in a test of 400 georegistrations against both NAIP orthoquads and orthorectified World View 2 imagery, the mean error was 4.56m; far worse than what is required to perform multispectral analysis with pixels covering less than 5cm.

This test of mosaics derived from SIFT made it readily apparent that the images could not be made spatially accurate without incorporating triangulation in the mosaicking process (Strecha). If the image sets from the two cameras were not going to be combined, however, Microsoft ICE could be used to derive information, which is then correlated against another more spatially accurate sources, by performing some manual interpolation based upon relative positions. The ability to perform multispectral analysis mandated that both the RGB and NIR datasets be as close to a pixel-to-pixel match though, because any differences between the two will induce error.

The accuracy test was conducted using the NIR and red images compiled in ICE by geo-registering the two against both 1m NAIP and .5m

panchromatic WorldView 2 imagery. 20 points were used to register the images in five separate attempts, resulting in 400 data points in total. Each of those data points being the root mean square error (RMS) in meters, between the accepted standard of NAIP or WV2, and the image created in ICE.

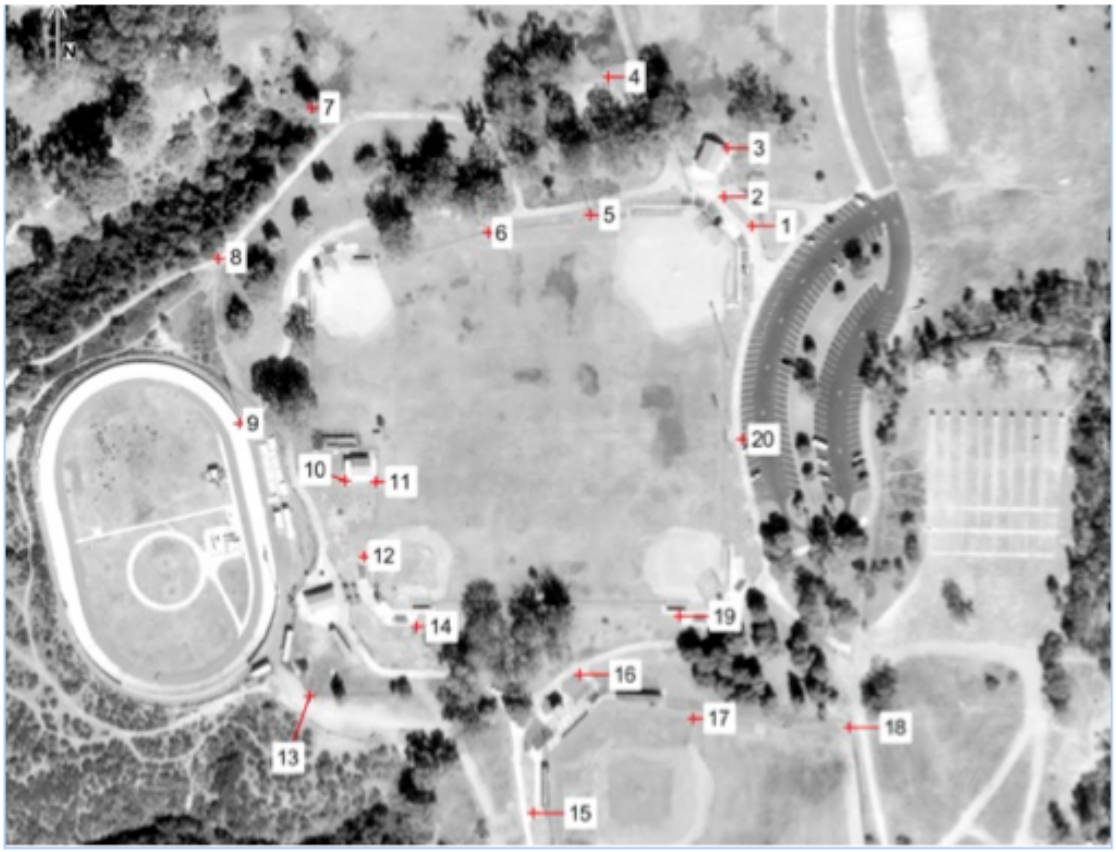

Image 3.0.0: WorldView1 image annotated with 20 points used for georegistration in accuracy testing of ICE and Pix4D mosaics

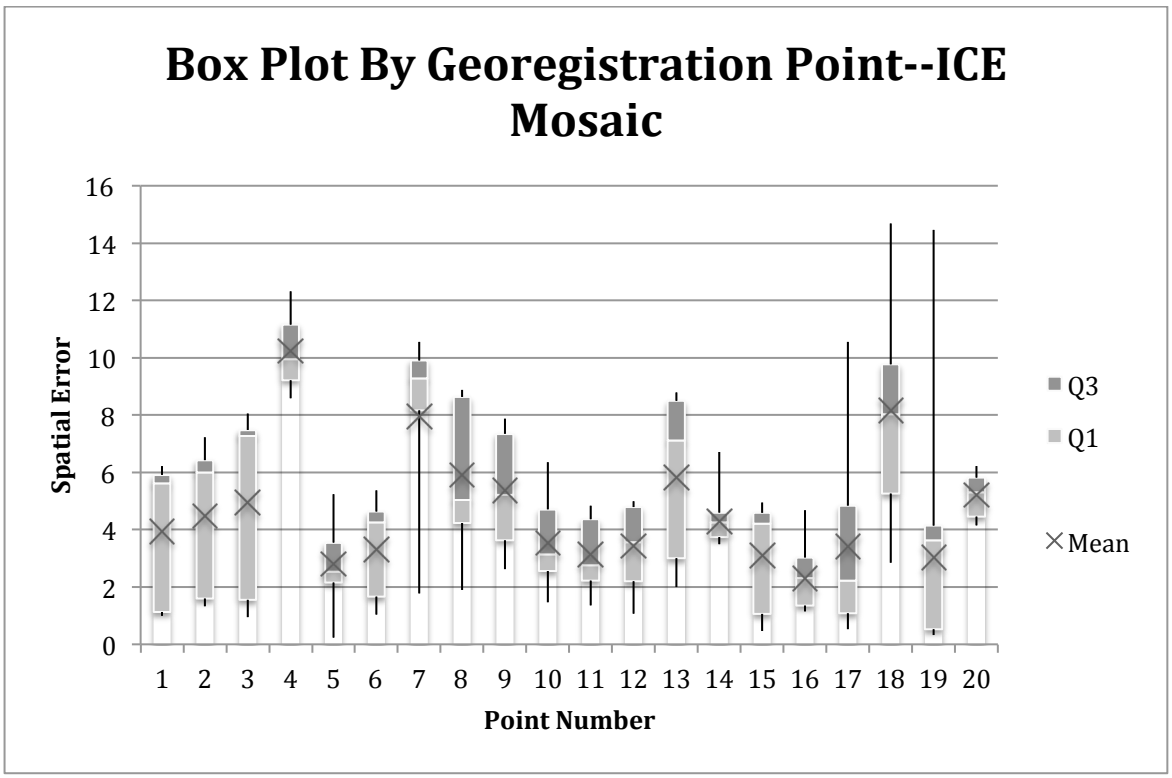

Chart 3.0.1: Spatial accuracy (in meters) of a georegistered ICE mosaic

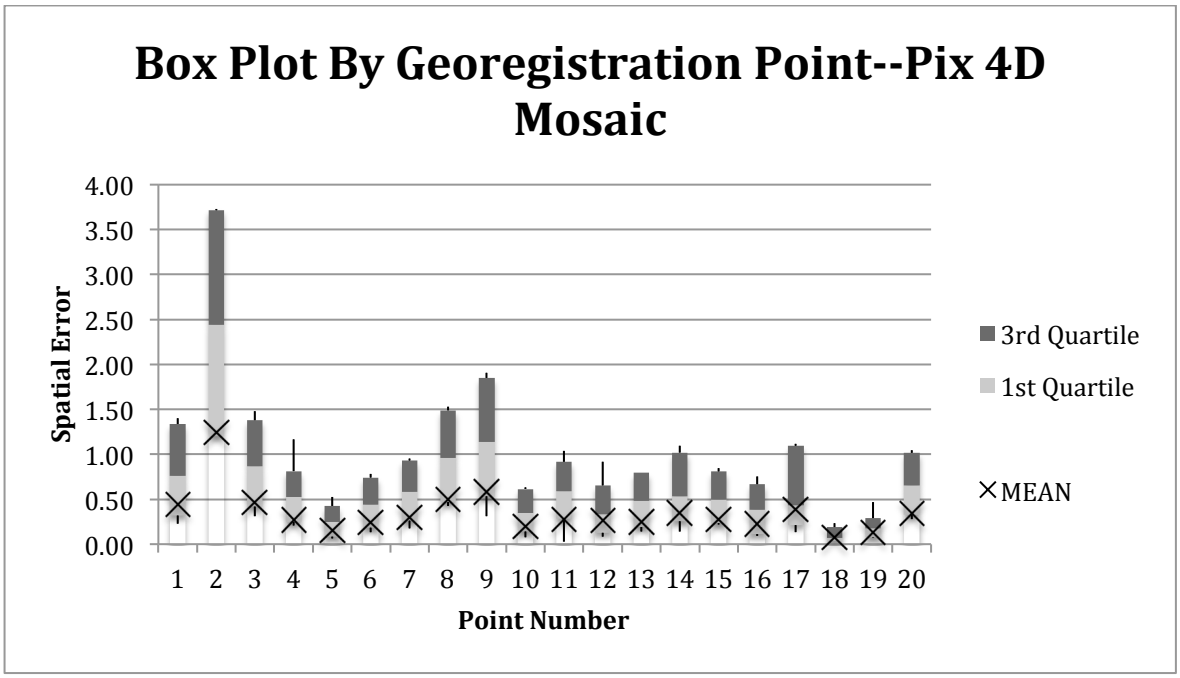

Chart 3.0.2: Spatial accuracy (in meters) of a georegistered Pix4D mosaic

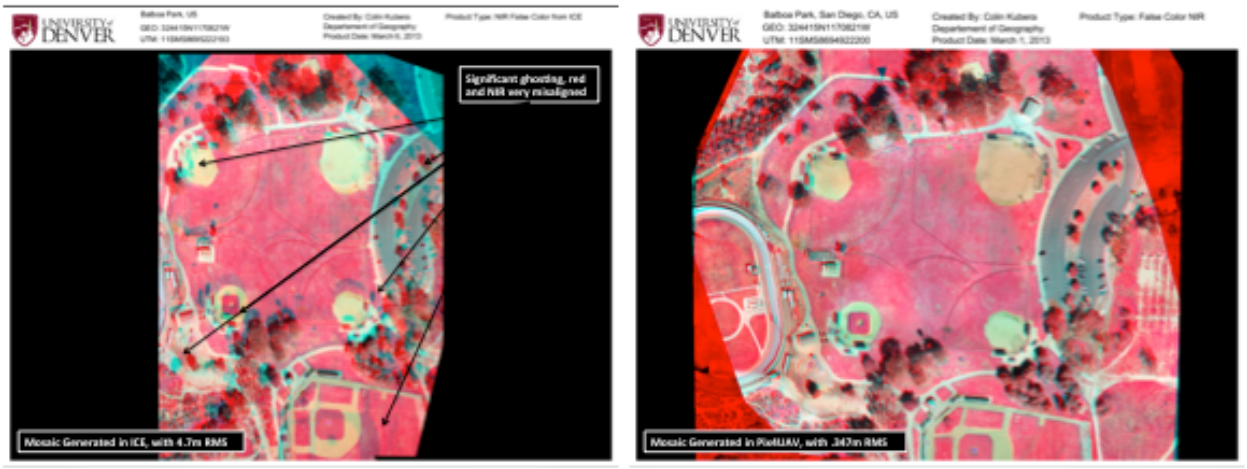

Image 3.0.1: Color infrared images created from ICE and Pix4D mosaics

This test was then repeated using the same 20 points and one mosaic created in Pix4D. With only a total mean RMS of 0.347m, it is plainly obvious that by using Pix4D for generating orthomosaics, the absolute accuracy can be brought almost to parity with the accepted standard. Having consistently accurate products is necessary for information that will be used for near-term decision making and in aiding future assessments by adding historical context by way of being archived in a geodatabase. Without this level of spatial accuracy, it would not be possible to perform reliable multispectral analysis, as it is particularly critical for separate bands to align.

Multispectral Analysis

Also during the first phase processing, it was quickly realized that the cameras should be identical so that the images could be taken at the same rate, respond similarly to each scene, and with the same image footprint. Testing was initially conducted with a modified Canon A495 for NIR and a Canon 780IS for RGB, but the RGB camera collected images at a slower

rate, resulting in voids in the early mosaics. Once a second A495 was acquired, testing was conducted with an Xnite-630nm filter, so that only red light would arrive at the CCD (blocks visible light with wavelengths shorter than red light, but not NIR), rather than extracting the red band from the RGB image. This effort proved futile though, because adding the filter caused the majority of the red images collected to be blurred and ultimately unusable. The only alternative solution would have been to also replace the IR filter from the second canon A495 with a red bandpass filter (blocks both all light of shorter and longer wavelength than red) in front of the lens, in the same way that the NIR camera uses a Hoya R72 filter to block any light below 720nm.

With both RGB and NIR image sets effectively captured and transformed into spatially accurate orthomosaics, multispectral analysis was performed using SOCET GXP 4.1 in order to merge the RGB and NIR images into a single multispectral container. These results were validated against those of WorldView2 imagery (four-band) that analyzed using the same parameters. The most important of the comparisons was using NDVI, which showed a much finer level of detail in the SUAS image analysis, as a result of the finer pixel resolution. Despite the promising comparison in result, it's not possible to definitively determine that the SUAS provides better analysis in this case, since the two images were captured years apart, nor (???) more

significantly because of the variance introduced by the difference in spectral sensitivity between the two sensors.

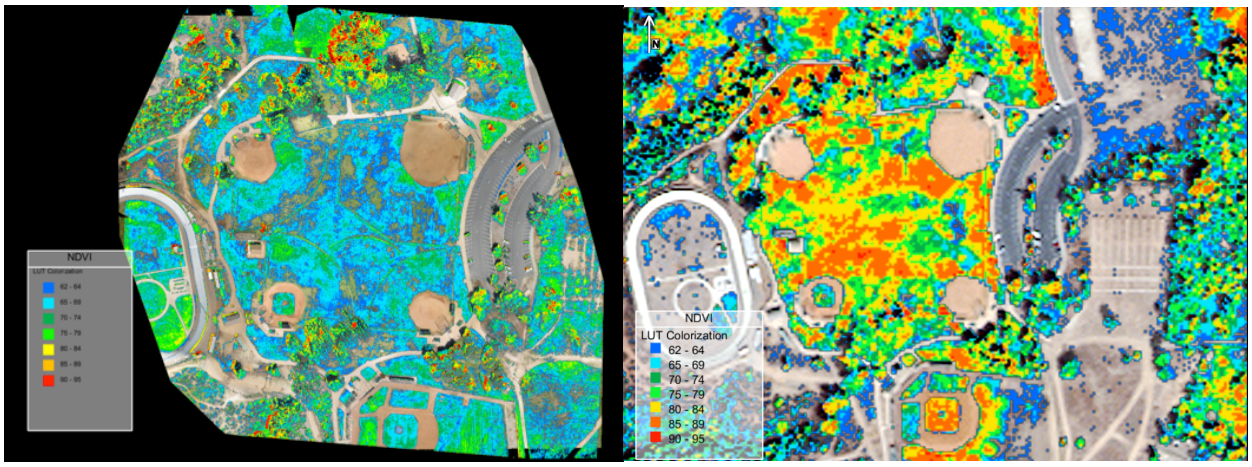

Image 3.0.2: Comparison of SUAS and WV2 NDVI

SOCET GXP's Find in Scene tool that matches spectral signatures was also used to compare the SUAS with WV2. The finer resolution was again readily apparent in the results, but both produced anomalous points that were not identified with the eucalyptus tree species used as a sample. Furthermore, neither of the Find in Scene results were verified with ground truth samples so there is no true measure of either's accuracy. Find in Scene can be a useful tool for surveying large areas for a particular species or substances, and even with some false points, the SUAS imagery appears to be nearly as capable as the four-band WV2 imagery in this role.

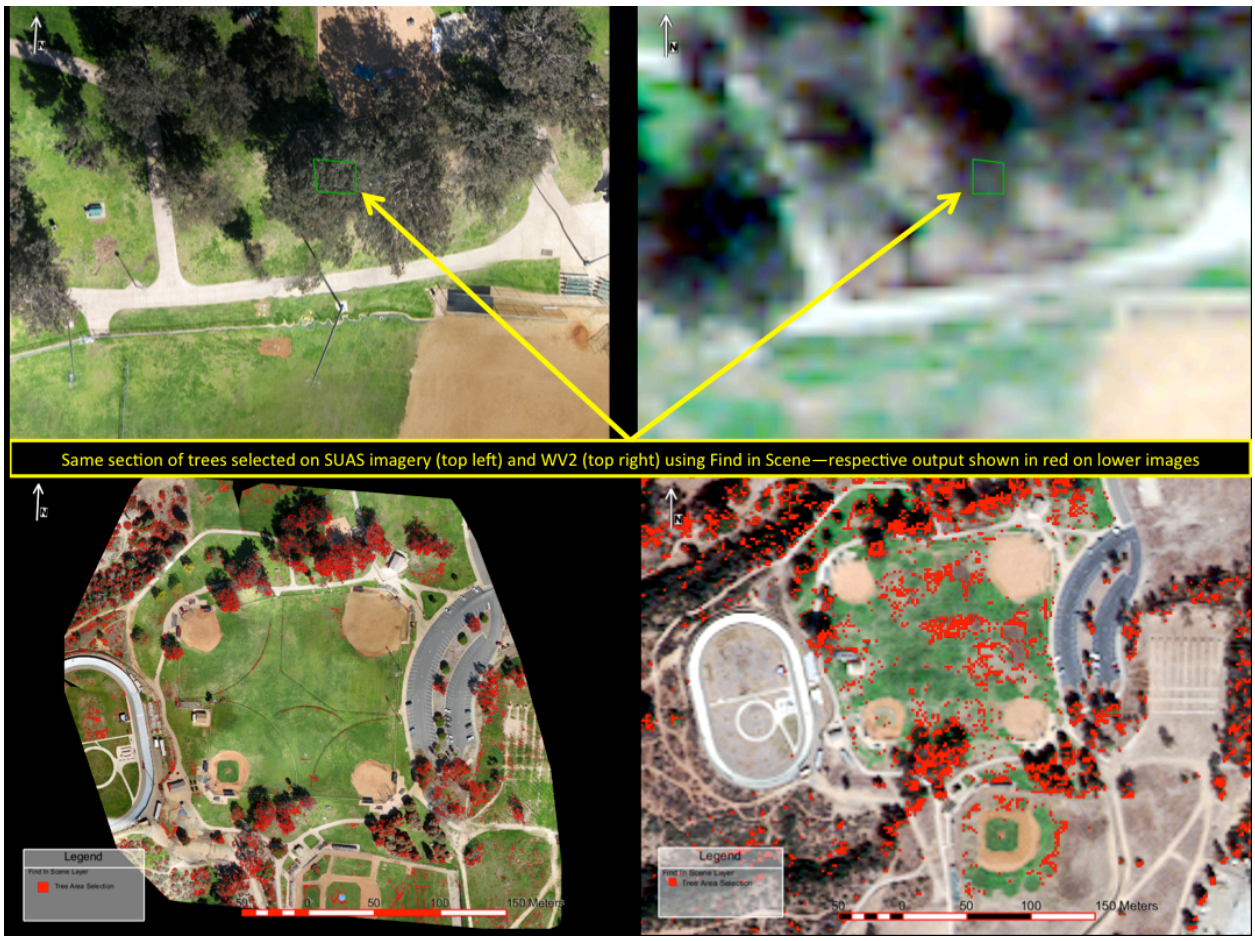

Image 3.0.3: SUAS and WV2 Find in Scene selection of eucalyptus trees

Discussion of Testing Results

Even though later testing showed sufficient overlap in the images as a result of adding altitude and slowing the aircraft to prevent voids in the mosaics, distortions were observed for taller objects, since they were not always acquired directly at nadir. In order to minimize the impacts of these distortions, the flight path was doubled in length by adding a complete secondary collection run perpendicular to the first passes over the area of interest. This redundant collection was essential to reducing distortions, and maximizing spatial accuracy though. If there were follow-on tests, it would

be worth reviewing whether this duplicate coverage resulted in significant changes in spatial and spectral accuracy.

Image 3.1.0: Pix4D orthomosaic with distortions from mosaicking process

Limitations

Even though the flight path can be planned to accommodate ample image overlap, execution can be limited if GPS accuracy is degraded. Planning can also prove to be flawed if the flight path does not extend more than one image length beyond the intended collection area, and if successive waypoints are closer than the SUAS can navigate. Poorly placed waypoints

can cause the SUAS to oscillate as it overcorrects and struggles to return to the intended route. When this happens, the images capture obliquity and therefore should not be used in the mosaic because they're likely to add distortion that will ultimately corrupt the results.

Another primary consideration with respect to operating parameters is wind. The exact effects vary depending on the platform; however, in conditions tested, winds less than 10 KTS generally had minimal impact. Winds greater than 10 KTS, especially with gusts, complicate collection though. Gusts in particular cause the SUAS to roll, again adding obliquity to any images collected while the SUAS counters the roll. Lastly, it must be considered that steady wind will cause certain legs of the flight path to be faster, and others slower. This difference in speed will both aid and challenge collecting sufficient image overlap.

With respect to the spectral accuracy of the camera, there is a lack of certainty in this experiment. Because neither of the cameras was validated with radiometric calibration on the ground or in flight with a test panel in the field, and since there were no in situ measurements taken with a different calibrate spectrometer, their sensitive wavelengths are based on assumptions. Additionally, the spectral bands are not narrow, as are those found on imaging platforms like WorldView 2 or an ADS-40, so spectral measurements are less precise and the exact identification of features in a particular scene is more challenging (Leica 2004).

Employment Scenario: Orfila Vineyard

In order to test the SUAS system in a real world scenario, the kind managers of Orfila Vineyard and Winery granted me permission to fly my RC-plane over their 35-acre property. The collection took place at 11:40am on April 10, 2013, approximately one hour prior to solar noon in order to minimize shadows and maximize the solar reflectance on the crops. The vineyard sits in North County San Diego, approximately 4 miles southeast of Escondido, CA, in the San Pasqual Valley. The weather was 70^{o}F, and wind was from the southwest at 9 mph with gusts above 15 mph. Only the southern field was imaged in this test for the respect of privacy of houses, which lie in close proximity to some of the other fields. The flight lasted 9 minutes from launch to recovery, with redundant overlap to ensure that all areas of the 10-acre field of interest did not have any collection gaps. Since the camera is controlled by an intervalometer script to collect images every three seconds, the chance of missing an area due to lack of redundant coverage is a very real threat, and would require a repeat flight to ensure comprehensive coverage.

Images collected

In the span of 7 minutes and 30 seconds that it took the RC-plane to fly the planned route (not including the time needed to climb and descend during launch and recovery), 129 RGB images and 150 NIR images were collected, covering approximately 17 acres. While each camera was set to

capture an image every three seconds, it's possible that the RGB camera was operating slightly slower than the NIR camera, as only a half-second difference would account for the difference of 21 images collected. It's also possible that RGB camera was more sensitive to the motion of the RC-plane and delayed taking pictures until it was in focus. In order to minimize distortion in the orthomosaic, the images that were noticeably non-nadir were deleted from the image directory, rather than leaving them for Pix4D to reject or attempt to force a poor solution for an oblique image. After deleting the non-nadir images, there were 86 RGB images and 119 NIR images remaining to be geotagged. Regardless of the initial difference in image count, more RGB images were rejected during the manual process of removing oblique images. This is likely attributable to the fact that it is easier to visually discern and interpret the RGB images, including their orientation, which made them more prone to be eliminated.

Geotagging

After removing the noticeably oblique images from the directory, the open source program GeoSetter was used to match the GPS file (.gpx) from the inertial navigation unit to the photos by synchronizing the time stamps of each. The onboard GPS records a data point every second, which is sufficient for processing a mosaic; however, these data points are prone to error, which is then translated to the images corresponding to those times,

potentially resulting in a particular image not being included in the mosaic, depending on the severity of the error.

Mosaic creation

With the photos' metadata updated to match a reasonably close camera position, the images were uploaded to Pix4UAV, using triangulation and SIFT to compile a spatially accurate orthomosaic (Strecha). The difference in the number of images used to generate the mosaics indicates that neither the raw images nor the derivate mosaics are absolutely identical. Consequently, each data set includes separate artifacts and errors in the mosaics.

Calculated Ground Sample Distance & Footprint of a Single Image

To calculate the resolution or Ground Sample Distance (GSD), the equation is as follows: GSD=(average height (AGL) x pixel size) / focal length. In this test scenario, the Canon A495 flown at 120m Above Ground Level (AGL) equates to 3.1 cm. An average height of 120m was established when the route was planned, and the focal length of the camera was known to be 6.6mm when not zoomed in. The pixel size was calculated by knowing the physical dimensions of the sensor, and the pixel count corresponded to these dimensions. The CCD sensor was physically 6.16mm x 4.62mm, with an array of 3648 x 2736 pixels, giving a pixel size of 1.69 E-6 m:

GSD = (120m x .00000169 m) / .0066 m = .0307m or 3.07cm

Using the calculated GSD, the image footprint can be calculated by multiplying the GSD by the number of pixels in the length and width of the CCD.

- Footprint length = 3648 x .0307m = 112m
- Footprint height = 2736 x .0307m = 84m

This footprint size was compared against a single image that was used in the mosaic, but registered independently, and measured to have a footprint of 115.6m x 78.1m. Since the calculation is dependent on an average height, the values are approximate for the particular image; however, the difference between the real-world and calculated values is negligible (3.12% and 7.55%, respectively), considering that there is also variance induced by the registration process.

Image: 4.0.0: Single frame image from SUAS registered to NAIP natural color image to depict the dimensions of a single frame

Registration

Because multispectral analysis is dependent on different image bands aligning exactly, both the RGB and NIR images were georegistered to an orthorectified World View 2 using the same identifiable points on all three images (Digital Globe). Second order registration was used and obtained a Root Mean Square Error of .44m for the NIR image and .38m for the RGB. This indicates that there were some latent differences between the two images that even at a half-meter of error, could result in the NIR and RGB images being misaligned, resulting in inaccurate spectral measurements. The problem of spatial error is exacerbated by having used two cameras, and by capturing images near-simultaneously, rather than at the exact same moment. This error could be reduced if the RGB and NIR sensors were integrated (such a sensor is commercially available from Tetracam).

Chipping

Once registered, SOCET GXP generates a supplemental (.sup) file to modify and improve the spatial accuracy of the original image. These two spatially corrected NIR and RGB images were saved back into their native GeoTiff format, with the Red component extracted and saved independently from the RGB image.

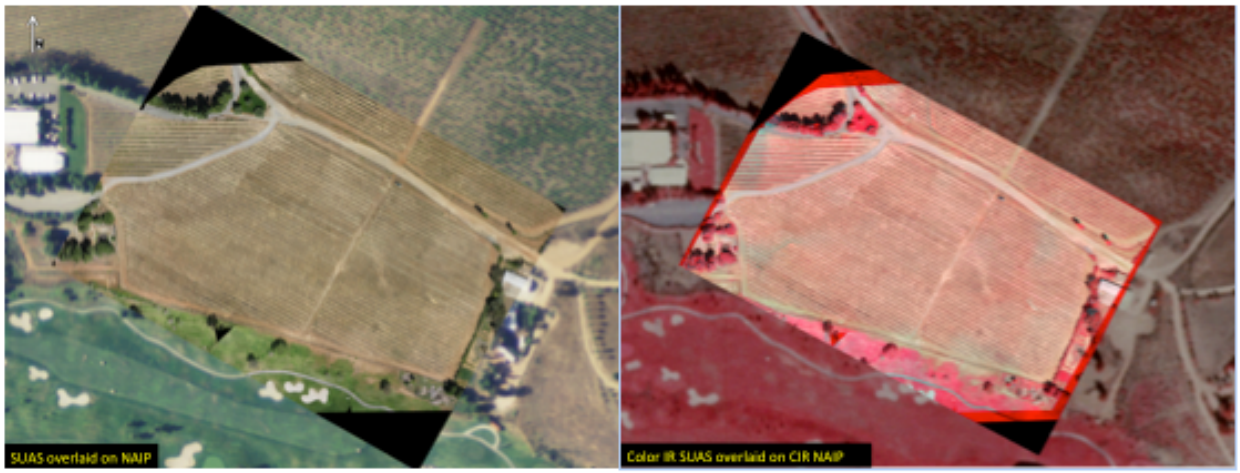

Image 4.1.0: Natural color and color IR Pix4D orthomosaics over NAIP

Multispectral Image Containers

Using the chipped images, two multispectral image (MSI) containers were created: one combining the NIR image with the RGB image, and the other combining the NIR with the Red band. Using the NIR and RGB container, the displayed red value was switched to display NIR, the green to display red, and blue to display green. The MSI container of red and NIR was used to run NDVI. Even though the images were not assigned metadata for their wavelengths, this process works because SOCET GXP is evaluating the digital numbers associated with the two bands for any given point.

NDVI Analysis

After running the spectral algorithm against the MSI container, colorization was applied and the bin ranges were adjusted to eliminate the noise, focusing instead on analyzing the variance in vigor of the vines. Any values below 65 were primarily associated with pavement and dirt within the

scene, and any values above 85 were largely attributed to grasses, trees, and some shadows. Regarding the values between 65-85, all of the vines had components within the 65-75 range, but the density of those values varied. Those values of 75-85 were only associated with those vines displaying the most vigor. Because the field was imaged so early in the season and the leaves on the vine had only recently bloomed, the vine leaves in the target field were still very small compared to those in adjacent fields and compared to the same field in mid to late season. Even while targeting the specific ranges of the vineyard, the low leaf density challenged analysis. The most vigorous growth in the scene was apparent on the western fields closest to the winery (appears on the left side of the imbedded images), where other grape varieties were growing.

The challenge of imaging small vines leaves was compounded by unevenly distributed vines. The particular block of the vineyard that was surveyed contains a mix of older and younger vines, where the younger vines were planted to replace older, low yielding vines. The exposed soil between vines created gaps in the health assessment, which could be interpreted wrongly without verifying the results. This underscores the importance of reviewing the results from NDVI against the original imagery, and possibly even reviewing the vigor assessment within the context of a geodatabase that archives age, health factors, and yield.

There were two additional areas within the field for, which analysis gave questionable results. In the southwest corner of the block there were vines that appeared to be more vigorous than the rest of the block. In this region there were dark spots that at first glance appeared to have been from local irrigation, or variances in the soil. These dark spots contributed to the highest NDVI values in the vineyard, which was the result of high NIR reflectance values from the vine leaves, and extremely low red reflectance from the dark patches on the soil. It was only after the vineyard manager clarified what the spots were that they could be deemed anomalous. The dark soil was actually mulch, formally known as pomace, made from post-fermentation grapes skins. The grape skins still contain high amounts of nitrogen and potassium, which are valuable for fertilizing the field (Dickerson 1996).

Image 4.2.0: Single frame image depicting vine row with pomace covering the ground

The other region that could not be accurately analyzed was on the eastern most portion of the field. That particular area appears blurred

because of the mosaicking process. It is probably the result of a bad geotag, for which Pix4D attempts to compensate for by placing the delinquent image in the location that it assesses to be the correct one. In spite of Pix4D's correction, the blurring in the RGB image prevents the correct values from running in NDVI and therefore reduces the reliability of the results.

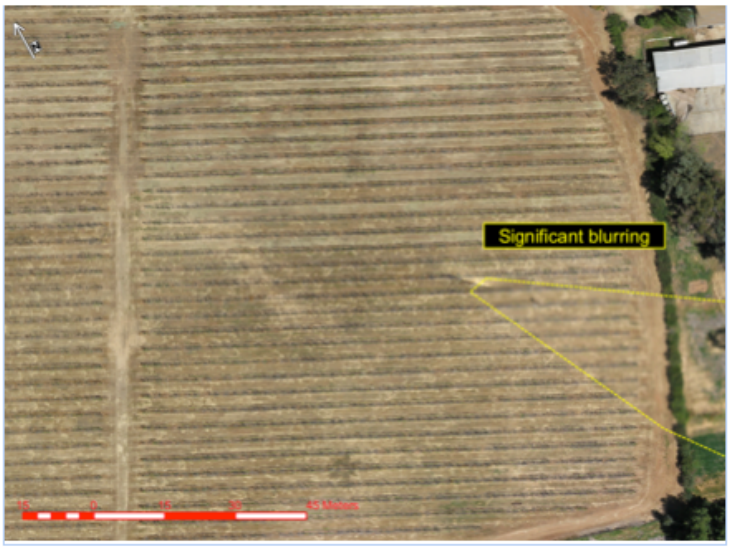

Image 4.2.1: Portion of Pix4D orthomosaic depicting blurred area on Eastern border of the field

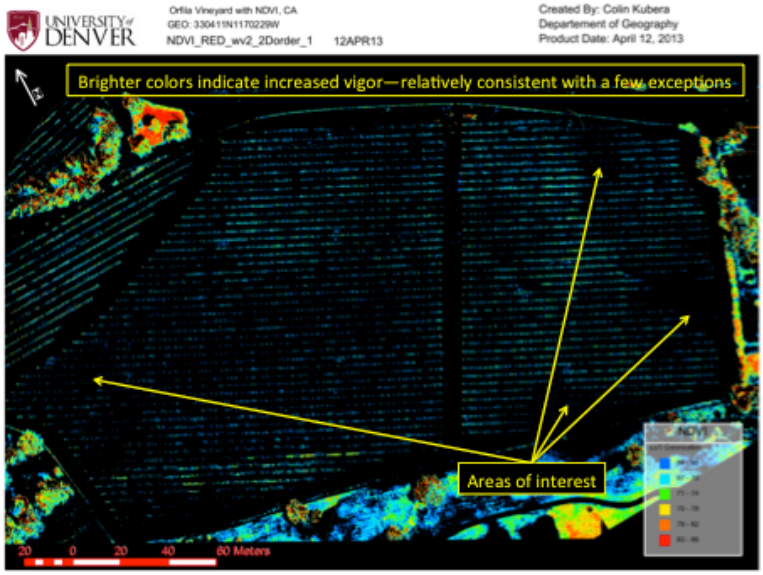

Image 4.2.2: NDVI results showing four distinct regions of low vigor

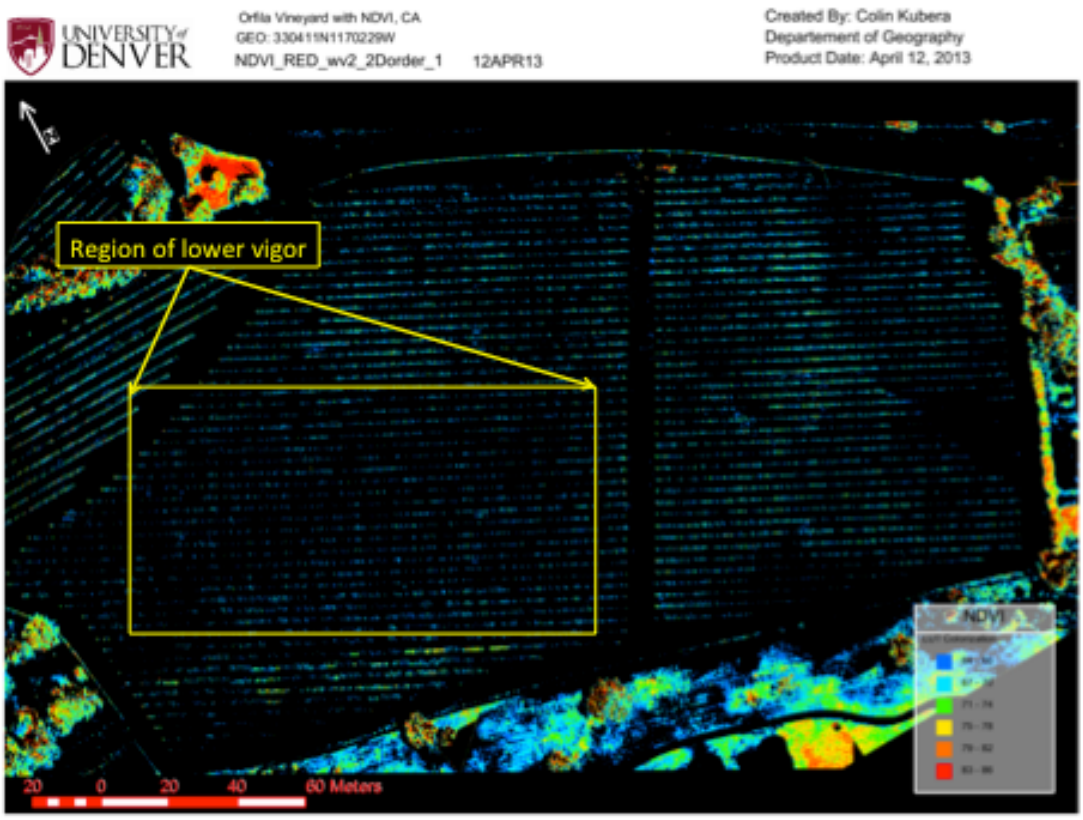

Image 4.2.3: Largest general region of low vigor shown in NDVI analysis

Effect of Shadows

Similar to the dark spots of pomace, shadows may also lead to false interpretations of plant vigor. The areas of highest vigor in the scene were the result of shadows in every case. This complication of artificially inflated values was strongest in the locations where shadows from trees fell over healthy grass. While those highest areas could be effectively edited out by not permitting the highest NDVI values to display, there were still similar, but weaker values within the vineyard that could not be removed without influencing the values displayed for the vines. Rather than exposed dirt

between the vines, there was cut grass, which was dead at the time of imaging, covering the ground between vine rows. The dead grass had a higher NIR reflectance than bare soil, and when in the shadow of the vine, the resultant reflectance value was similar to that of the vine leaves.

Despite the similar NDVI values, the large shadows, which were more visually significant than the leaves on the vine so early in the growing season, could possibly be used as a surrogate in determining health. However, if shadows were used to evaluate health instead of the vine leaves, then frequent collection at the same time of day would be necessary in order to measure changes in leaf area, to verify growth and ensure that leaves are not declining instead. Decline would be an obvious indicator of crop stress, but would still need to be verified by closely examining the vines, because of the variability in shadow length. The dynamic length of shadows would also dictate that the solar elevation and azimuth are as similar as possible between collections, because otherwise the comparison of shadows would lead to erroneous conclusions about health and growth.

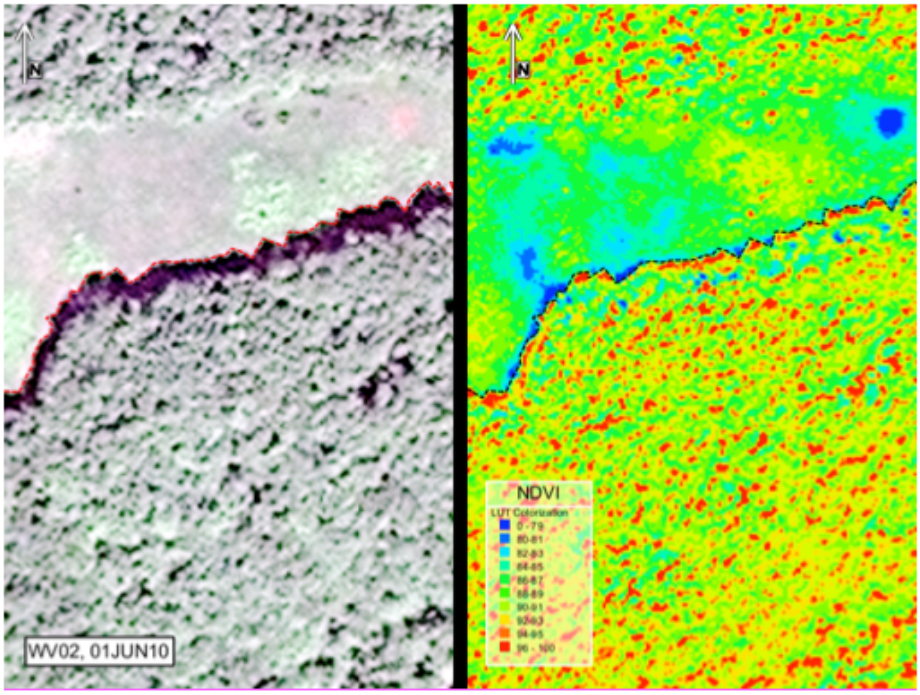

Image 4.3.0: Natural color WV2 image with its corresponding NDVI output demonstrating higher than expected results from NDVI in shadow along a tree line

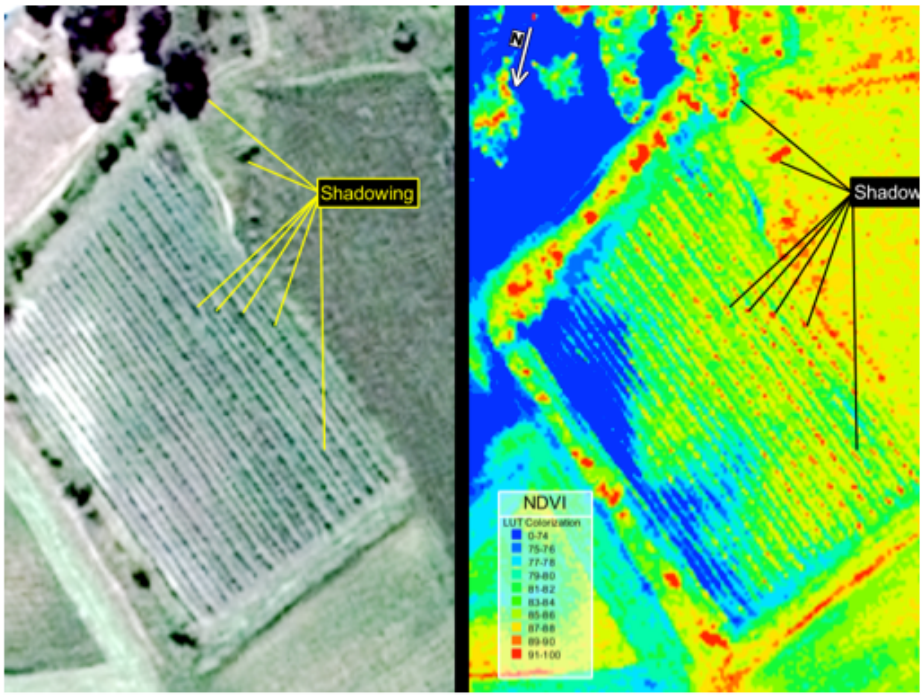

Image 4.3.1: Natural color WV2 image with its corresponding NDVI output demonstrating higher than expected results from NDVI due to shadowing in a vineyard

If time were not a factor in the research behind this paper, the study would continue through harvest with multiple collections performed on at least a monthly basis. And if money were also not an issue, all of the collections would be compared with in situ spectroscopy and GPS point collection to validate the spatial accuracy of the method tested.

Although the vine leaves were smaller than ideal for evaluating their health, their diminutive size presented a separate parallel test scenario for the complexities of detecting noxious weeds among crops (Torres-Sanchez et al 2013). If a SUAS were tasked with identifying weeds, the target plants might be similar to the vines in the test scenario, because of their small physical size within the scene, even when clustered together. While it was possible to detect vines versus other types of vegetation in the scene by using SOCET GXP's Find in Scene function in an MSI container, the wide spectral bands of the SUAS's sensors used in this case are not as effective as remote sensing-specific sensors. Some companies like as Tetracam, manufacture SUASs purpose-built sensors, and have bandwidths designed to emulate to those of Landsat. However, the Landsat NIR band is still less focused than either the ADS40 or WorldView2 and could therefore still struggle to identify thriving weeds dispersed among crops (Tetracam). One possible alternative, both in the application of detecting weeds and imaging small vine leaves would be to fly lower to increase image resolution,

however in this specific test that would have led to less image overlap and possibly a lower quality orthomosaic.

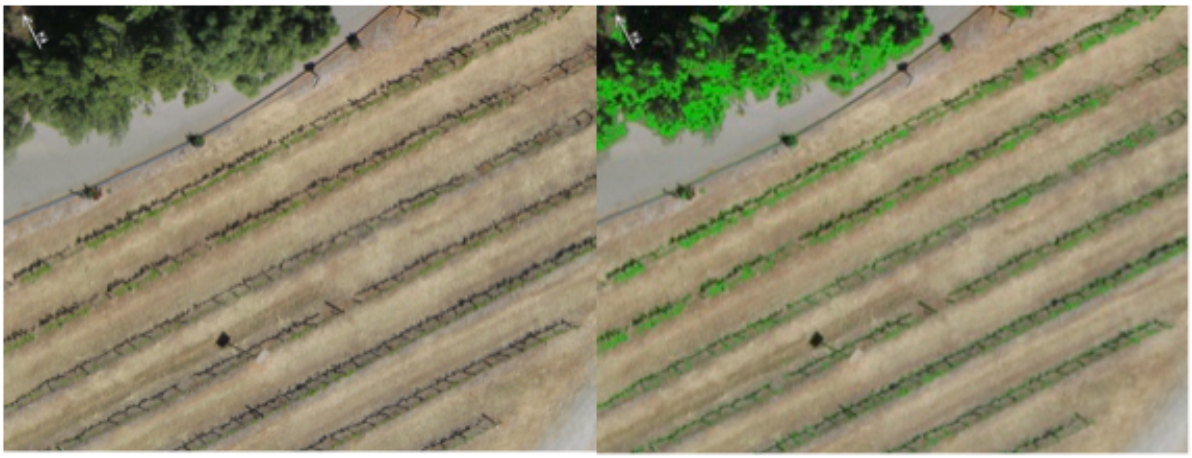

Image 4.4.0: Natural color image displayed with NIR merged in the image (band not shown) and Find in Scene selection in green from selecting a vigorous point on the vine

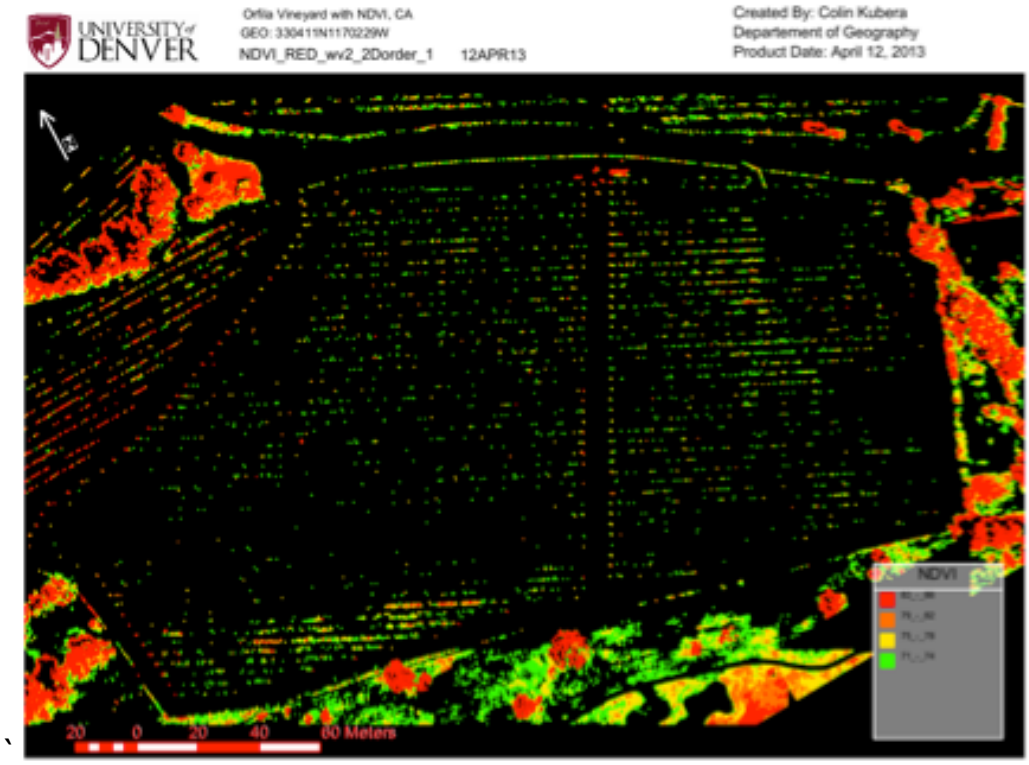

Image 4.4.1: Vectors generated from a Find in Scene selection of the highest vigor vines.

Incorporating Raster Data into a Geodatabase

Using the raster data from either Find in Scene or NDVI, SOCET GXP can convert the results into vectors so that the data can be fully utilized within other GIS applications like ArcMap. Archiving the data in the context of a geodatabase is when it would become most beneficial as it establishes a baseline of normal and expected behavior between seasons. This baseline understanding of penology is exactly what is necessary to advance farming management from a field or block level down to a sub-field or sub-block approach.

Implementing a geodatabase for vineyard management would start with several rectangular shapefiles joined end-to-end, to represent the location of vine. The database might only start with a vine ID, the type of grape, and age of the vine, but the database would quickly be populated with data from treatment and health monitoring. Using the data generated in GXP and simple overlay analysis in ArcMap, the NDVI values can be brought into the Geodatabase to categorize the vigor each vine. The presence of disease and pests could also be entered along with any corresponding treatment options for individual vines. All of these data points could then be used to predict the yield for a season, or to determine where the highest quality grapes are located within the vineyard for a particular reserve or select label bottle of wine.

Currently, the Orfila Winery tracks its harvest yield by block, however, it could be beneficial to track it at a sub-block level to track the origins of the highest quality grapes. This cannot be accomplished by blindly dividing the blocks equally though. Instead, by imaging the vineyard at veraison (when the grapes stop growing, change color, and begin to ripen) the plant vigor at that stage can be used as a predictor of yield for that season (Lamb et al). By subsequently confirming the yield from those areas of higher and lower vigor, the performance of individual vines can be tracked and used in the planning of future wine batches, or to evaluate the success of previous image collections to refine the accuracy of the data derived from the analysis.

Orfila applies its fertilizing regiment evenly across its fields with irrigation. The success of the Farmstar and Oenoview programs have demonstrates the value of individually tailored assessments for future nitrogen application, because by prescribing specific subfield applications, the total amount of fertilizer consumed by their subscribers was reduced (BordeauxWineNews). In time, the technology may evolve enough so that the same will be true for pesticides. Both Farmstar and Oenoview are satellite imagery based programs though, and as already discussed, satellite imaging tends to be expensive. The Oenoview program claims to only cost its subscripers one Euro-cent per bottle—a minor cost which could easily be

passed on to the wine consumers while enhancing the quality of their wine (Douche et al).

Adopting SUASs in the United States for Civil Aviation:

While the United States lags behind Europe and Japan in its implementation of SUASs, the number of agencies and universities seeking formal approval from the FAA for authorization to operate is growing rapidly. The USGS and Utah Water Research Labs are currently leading the way in non-military applications for SUASs in the US. The USGS has already employed the SUAS fleet to investigate various habitats, monitor for erosion and invasive plant species, and even inspecting mines (USGS UAS Program Office). This diverse mission set is an example of the wide and varied applications that SUASs can and will be involved in, so it is unsurprising that the forecasted economic benefit from adopting SUASs is so massive—over 100,000 jobs are expected to be created, bringing $13.6 billion in economic growth by 2025 (Dillow 2013). The on demand capability of SUASs will give users far greater control in tasking image collection, and will revolutionize commercial remote sensing. With such a forecasted boom in remote sensing, because of SUASs, the GIS industry will be directly affected, and will need to prepare for the added demand for GIS expertise, just as the FAA will need to prepare to deal with more congested airspace at low levels.

Conclusion:

For many reasons, this test does not achieve a one-to-one comparison to satellite and traditional aerial collection, and chiefly among those is because image acquisition from the two cameras was not simultaneous, and nor were the cameras calibrated to verify the wavelengths captured by each. In spite of these major differences, and slight variances in initial image processing, SUAS derived imagery has proven that it can be used as an effective substitute to traditional collection methods at small scales.

Since the flight times of SUASs are so limited, they cannot possibly compete with satellites in imaging large areas in distant locations, because imaging satellites are by strict definition remote sensing systems that provide global coverage in just over a day's time. Furthermore, the raw images collected by SUASs have very limited spatial accuracy, due to the relatively rudimentary positioning systems on board the SUAS, unlike those associated with satellites and modern commercial cameras flown on manned aircraft. Lastly, attrition rates will likely be far greater with SUASs unless they are operated with some standard of formal training for their operators, and safety specifications for the platforms.

Even with the inherent limitations of SUASs though, they will likely become the go-to tool for farmers to monitor their crops on a micro scale. And despite the progress of the National Agriculture Program with respect to the resolution and currency of imagery that it is providing, relatively

infrequent collection will continue to hinder its utility for the individual farmer. The most significant obstacle that would prevent a farmer from employing SUASs on their own will likely be the cost of the software licenses needed to perform spatial and spectral analysis, so it is more likely that a select few companies will operate SUASs, just as is the case with traditional aerial imaging. However, because the operating costs of the SUAS are almost negligible, individual farmers may soon be able to afford tailored imagery collection because of the SUASs. This project demonstrates that it is possible for SUASs to achieve near-parity with existing commercial platforms in spatial accuracy when processed correctly, and can far exceed the capabilities of those systems in image resolution (GSD) and revisit rate, to rapidly survey multiple fields at a local level.

Works Cited

2007 Census of Agriculture County Profile: San Diego County California. USDA. http://www.agcensus.usda.gov/Publications/2007/Online_Highlights/County_Profiles/California/cp06073.pdf (Accessed April 1, 2013).

2012 HIFLD (homeland Infrastructure Foundation—Level Data) Working Group. Sept 13 2011. http://www.fsa.usda.gov/Internet/FSA_File/hifld_sep_2011_naippdf.pdf (Accessed April 1, 2013).

Astrium EADS. "Ploughing a Better Furrow." 25 Nov 2011. http://www.astrium.eads.net/en/articles/ploughing-a-better-furrow.html (Accessed 20 Apr 2013).

Barrie, Allison. "Utah Water Research Lab Drone Fleet." Utah State University College of Engineering. http://www.engineering.usu.edu/htm/news/articleID=17052 (Accessed 27 April 2013).

BordeauxWineNews. "Viticulture: Cheateau De Fieuzal Under the Satellite." August 10, 2009. http://bordeauxwinenews.blogs.sudouest.fr/tag/Oenoview (Accessed April 25, 2013).

City of San Diego. Economic Development: Population. March 1, 2011. http://www.sandiego.gov/economic-development/sandiego/population.shtml (Accessed April 1, 2013).

Canon Hack Development Kit. Chdk A495. June 5, 2011. http://chdk.wikia.com/wiki/A495 (Accessed July 25 2012).

Dickerson, George. "Mulches for Gardens and Landscapes." New Mexico State University. College of Agriculture and Home Economics. June 1996. http://aces.nmsu.edu/pubs/_h/H-121.pdf (Accessed April 20, 2013).

Digital Globe. Tuscany, Italy, 10JUN01102517-S2AS_R2C1-SIEN-nitf_I002682_FL02-P006470. WorldView 2, Multispectral. June 1, 2010.

Digital Globe. San Diego, CA, 02NOV09WV021300009NOV02183956-M1BS_R3C1-052565412010_01_P003. WorldView 2, Multispectral. Nov 2, 2009.

Digital Globe. San Diego, CA, 10APR08WV011300008APR10182351-P1BS_R1C1-052565744010_01_P002. WorldView 1. Panchromatic. April 10, 2008.

Digital Globe. San Diego, CA, 08FEB09183134-P1BS_R4C1-052565744010_01_P001. WorldView 1. Panchromatic. Feb 9, 2008.

Digital Globe. San Diego, CA, 24NOV09WV011300009NOV24184547-P1BS-052287262010_01_P001. WorldView 1. Panchromatic. Nov 24, 2009.

Digital Globe. "World View-2 Data Sheet." January 2013. http://www.digitalglobe.com/downloads/WorldView2-DS-WV2-Web.pdf (Accessed April 10, 2013).

Digital Orthophoto Quarter Quadrangles (DOQQ). Louisiana State University Atlas. May 14 2009. http://atlas.lsu.edu/doqqhelp/ (Accessed April 1, 2009).

Dillow, Clay. "What is the drone industry really worth?." CNN Money. March 12, 2013. http://tech.fortune.cnn.com/2013/03/12/what-is-the-drone-industry-really-worth/ (Accessed 27 April 2013).

Douche, Henri, V. Lefevre, H. Poilve. "Oenoview: Bringing Remote Sensing to Wine Quality." http://core.icpaonline.org/finalpdf/abstract_133.pdf (Accessed April 25, 2013).

National High Altitude Photography Program (NHAP). Department of the Interior, US Geological Survey. Feb 4, 2011. http://eros.usgs.gov/#/Guides/nhap (Accessed April 1, 2013)

Fate, Josh. "Canon A495 Specifications." http://www.steves-digicams.com/camera-reviews/canon/powershot-a495/specifications-49.html (Accessed April 27 2013).

Fletcher, Reginald S, Mani Skaria, David E. Escobar and James H. Everitt. "Field Spectra and Airborn Digital Imagery for Detecting Phytophthora Foot Rot Infections in Citrus Trees." HortScience. 36(1):94-97. 2001.

GeoSetter. February 1, 2011. http://www.geosetter.de/en/ (Accessed December 5, 2012).

Hoya Filters. "Infrared R72 Filter." http://www.hoyafilter.com/hoya/products/specialeffectsfilters/infraredr72rm90/ (Accessed July 25, 2012).

Johnson, LF, D F Bosch, D C Williams, B M Lobitz. "Remote Sensing of Vineyard Management Zones: Implications for Wine Quality." Applied Engineering in Agriculture. Vol 17(4): 557-560.

Jones, Hamlyn G, Robin A Vaughan. *Remote Sensing of Vegetation.* Lexington: Oxford UP, 2010.

Kempeneers, P, S DeBacker, PJ Zarco-Tejada, S Delaliuex. "Stress Detection in Orchards with Hyperspectral Remote Sensing Data" *Remote Sensing for Agriculture.* Vol 6359 (Oct 2006).

Lakehead University. "Lecture 7." flash.lakeheadu.ca/~forspatial/2270/**lecture7**/**lecture7**.pdf (Accessed April 1, 2013)

Lamb, David, Andrew Hall and David Louis. "Airborne Sensing of vines for Canopy variability and productivity." http://www.pvts.net/pdfs/ndvi2/NDVI_LAMB1.pdf (Accessed 10 April 2013).

Lebougeois, Valentine, Agnès Bégué, Sylvain Labbé, Benjamin Mallavan, Laurent Prévot and Bruno Roux. "Can Commercial Digital Cameras be used as Multispectral Sensors? A Crop Monitoring Test." Sensors. 2008, 8, 7300-7322.

Leica. "ADS40 Airborne Digital Sensor." 2004. http://www.dlr.de/os/Portaldata/48/Resources/dokumente/ads40_flyer_leica.pdf (Accessed April 1, 2013).

Leica. "PremierGeo Buys Third Leica ADS Sensor to Expand Airborne Imaging Capacity." February 26, 2013.

http://www.leica-geosystems.us/en/News_56320.htm?id=4374 (Accessed 11 April 2013).

Leica. "Monitoring Farmland Activies with the ADS40." 2004. http://www.leica-geosystems.com/en/Monitoring-Farmland-Activities-with-the-ADS40_4626.htm (Accessed April 20 2013)

Michael, Cannon. University of California Davis Precision Agriculture Workshop. "Site-specific management at Bowles Farming Company." July 14, 2010. http://ucanr.org/sites/paica/files/36939.pdf (Accessed April 10, 2013).

NAIP 2012. Escondido, CA. C33117a1ne.tif. Color-NIR. June 10, 2012.

NAIP 2012. San Diego, CA. ortho_1-1_1n_s_ca073_2012_1.sid. Natural Color. June 28, 2012.

National Aeronautics and Space Administration. "Landsat: The Thematic Mapper." May 9, 2013.

http://landsat.gsfc.nasa.gov/about/tm.html (Accessed May 10, 2013).

Pinot Growers Journal. "Mulching the Vineyard." 2006. http://kloppranch.wordpress.com/2006/12/21/mulching-the-vineyard/ (Accessed 20 April 2013).

San Diego Farm Bureau. "San Diego County Agriculture Facts." http://sdfarmbureau.org/SD-Ag/Ag-Facts.php (accessed April 1, 2013).

Statewide Mapping Advisory Committee. "Using Color Infrared" July 2011. http://www.ncgicc.com/portals/3/documents/using_color_infrared_imagery_20110810.pdf (Accessed April 10, 2013).

US Department of Agriculture (USDA). "National Agriculture Imagery Program (NAIP) Information Sheet." April 2012. http://www.fsa.usda.gov/Internet/FSA_File/naip_2012_infosheet.pdf (Accessed April 1, 2013).

Tetracam Digital Camera and Imaging Systems. ADC Lite. http://www.tetracam.com/adc_lite.html (Accessed April 1, 2013).

Torres-Sanchez, Jorge, Francisca López-Granados, Ana Isabel De Castro, José Manuel Peña-Barragán. "Configuration and Specifications of an Unmanned Aerial Vehicle (UAV) for Early Site Specific Weed Management" March 6 2013. http://www.plosone.org/article/info%3Adoi%2F10.1371%2Fjournal.pone.0058210 (Accessed April 15, 2013).

USGS UAS Program Office. U.S Department of the Interior. April 18, 2013. http://rmgsc.cr.usgs.gov/UAS/ (Accessed 27 April 2013).

Utah State. "Near Infrared Tutorial." March 2010. http://extension.usu.edu/nasa/htm/on-target/near-infrared-tutorial (Accessed April 21, 2013).